CrossMark
click for updates

A cobalt(II) spin-crossover compound with partially charged TCNQ radicals and an anomalous conducting behavior†

Xuan Zhang,[a] Zhao-Xi Wang,*[b] Haomiao Xie,[a] Ming-Xing Li,[b] Toby J. Woods[a] and Kim R. Dunbar*[a]

The bifunctional salt [Co(terpy)$_2$](TCNQ)$_3$·CH$_3$CN (terpy = 2,2′;6′,2″-terpyridine, TCNQ = 7,7,8,8-tetracyanoquino-dimethane) exhibits a high room temperature conductivity of 0.13 S cm^{-1} and an anomaly in conductivity at ∼190 K as evidenced by variable temperature structural, magnetic and conductivity studies. The anomaly in the conductivity at 190 K has been correlated with the temperature dependent structural breathing and Jahn–Teller distortion of the low spin state of the SCO units, as well as the charge fluctuations and supramolecular π-stacking interactions of partially charged TCNQ radicals. The modular synthetic approach leads to an accessible source of partially charged TCNQ radicals for the facile preparation of bifunctional molecular materials with high electrical conductivity.

Hybrid inorganic–organic materials are attractive owing to the flexibility in the choice of building blocks with tunable functionalities and their potential applications in memory devices and field-effect transistors.[1] An important subset of these materials is magnetic molecule-based compounds that hold promise for significant miniaturization of future devices.[2] Crystalline molecular materials are also advantageous for engendering multifunctionality through the use of modular synthetic procedures which is an ideal approach for building structure–property relationships.[3] Some notable examples are conducting magnets exhibiting bulk/single-molecule magnetic properties[4] and electrically conducting spin-crossover (SCO) complexes.[5]

The electron acceptor TCNQ (TCNQ = 7,7,8,8-tetracyano-quinodimethane) forms a highly stable radical which has been widely used as a building block for the design of coordination polymers and charge-transfer complexes with intriguing redox, magnetic, electrical conducting and/or switching properties.[6] The successful realization of molecular organic conductors requires the uniform stacking of organic molecules in addition to the presence of open-shell radicals, preferably with non-integer charges, and minimal coulombic interactions.[7] In TCNQ-based electrical conducting charge-transfer compounds, the TCNQ radical anions typically stack in a parallel manner,

a situation that facilitates overlap between their frontier orbitals. A main challenge that remains to be addressed, however, is the design of TCNQ-based multifunctional materials that exhibit synergistic interactions, rather than the typical scenario in which the properties are observed as isolated events in separate thermal regimes.[8]

Spin-crossover is a form of magnetic bistability triggered by external stimuli *e.g.*, light, pressure and temperature.[9] Given that crystal packing constitutes a chemical pressure which affects metal–ligand bond distance variations that occur with spin-crossover events,[10] we were curious as to whether these stimuli-responsive structural changes would affect the electron transport properties of a hybrid material that contains semi-conducting π-stacks of TCNQ radicals co-crystallized with a metal complex that undergoes notable structural changes under thermal perturbation. The underlying reasoning is that the transition temperature of the SCO event could be tuned over the temperature range of 100–300 K to match the thermal regime of the semiconducting behavior of the TCNQ sub-lattice.[6o,9c,11] In this context, we note that composite conducting SCO materials exhibiting synergistic interactions have been obtained by combining conducting organic polymers and SCO complexes.[12] A number of crystalline conducting SCO materials have also been reported which offer an ideal platform for the investigation of structural–property relationships by the co-crystallization of Fe-based SCO complexes with metal dithiolate radicals.[5a,10a,13] In order to realize significant electrical conductivity in these materials, however, galvanostatic oxidation of the mono-anion radicals is usually performed to generate partially charged radicals, which helps to enhance the delocalization of electrons throughout the radical stacks. In comparison, reports

[a]Department of Chemistry, Texas A&M University, College Station, TX 77842-3012, USA. E-mail: dunbar@chem.tamu.edu

[b]Department of Chemistry, Innovative Drug Research Center, Shanghai University, Shanghai 200444, P. R. China. E-mail: zxwang@shu.edu.cn

† Electronic supplementary information (ESI) available. CCDC 1049086–1049089 and 1426087–1426088. For ESI and crystallographic data in CIF or other electronic format see DOI: 10.1039/c5sc03547c

on TCNQ-based SCO conductors have been scarce, with the most recent one being reported by Shatruk and coworkers who took advantage of the comproportionation reaction between neutral TCNQ and the mono-anion TCNQ$^{\cdot-}$ radical to yield partially charged radicals which give rise to a high room temperature conductivity of 0.2 S cm^{-1}.[14] However, due to the extra step of combining equal equivalents of the two TCNQ sources in this comproportionation method, a single source of partially charged TCNQ radicals would be more convenient. In this vein, we noted that Gutierrez and coworkers reported the salt [Et$_3$NH](TCNQ)$_2$ as a source of partially charged TCNQ radicals for a series of electrical conducting compounds, viz., [M(terpy)$_2$](TCNQ)$_3$ (M = Ni, Cu, Zn). Unfortunately no structural information is available for these compounds.[15]

Recently, we reported the incorporation of TCNQ radicals into the SCO salts [Co(pyterpy)$_2$](TCNQ)$_2$·solvents (pyterpy = 4′-(4′′′-pyridyl)-2,2′:6′,2′′-terpyridine) and studied the effect of supramolecular stacking interactions of TCNQ$^{\cdot-}$ radicals on the structures and SCO behavior of the Co(II) entities.[16] As the temperature decreases from 300 to 110 K, an unusual structural "breathing behavior" was observed as the Co(II) coordination sphere exhibits a contraction from the HS-LS transition with subsequent expansion due to a Jahn–Teller distortion of the LS state of Co(II). However, due to the segregation of TCNQ radicals by the pyridyl groups of the pyterpy ligands, the conductivity of this material was not very remarkably high.

Herein we report the successful use of [Et$_3$NH](TCNQ)$_2$ as a readily accessible source of partially charged TCNQ radicals for the synthesis of the inorganic/organic hybrid bifunctional material, [Co(terpy)$_2$](TCNQ)$_3$·CH$_3$CN (**1**). This crystalline molecular material exhibits an impressively high electrical conductivity of 0.13 S cm^{-1} at room temperature due to the presence of partially charged TCNQ radicals despite their unusual "cross-stacking" patterns. In addition, the observation of an unprecedented anomaly in the electrical conductivity of **1** in the range of 180–190 K was observed which is attributed to the structural variations and charge fluctuations of the TCNQ stacks as evidenced by detailed temperature dependent X-ray crystallography, magnetic and electrical conductivity studies.

A facile metathesis reaction between [Co(terpy)$_2$](ClO$_4$)$_2$·0.5H$_2$O and the mixed-valence salt [Et$_3$NH](TCNQ)$_2$ in acetonitrile produces dark blue/purple thin needle crystals of **1** over the course of several minutes. Variable temperature single crystal X-ray studies revealed that the structure of compound **1** remains in the non-centrosymmetric space group *Pna*2$_1$ over the temperature range *T* = 300, 190, 180, 150, 130 and 100 K (Table S3†). The asymmetric unit of the structure is composed of one [Co(terpy)$_2$]$^{2+}$ cation, three TCNQ moieties and one free acetonitrile molecule (Fig. 1). The octahedral coordination environment of Co(II) is distorted in such a manner that the metal center is closer to one of the terpy ligands (N1N2N3) than the other one (N4N5N6). This is evidenced by the shorter bond distances of Co–N1 (1.867(3) Å), Co–N3 (1.980(4) Å), and Co–N2 (1.978(4) Å) than those of Co–N4 (1.920(3) Å), Co–N5 (2.153(4) Å) and Co–N6 (2.162(3) Å), as well as the larger bond angle of N2–Co–N3 (163.4(1)°) than that of N5–Co–N6 (158.0(1)°) (100 K, Fig. 2 and Table S1†). The Co–N1 bond distance is relatively
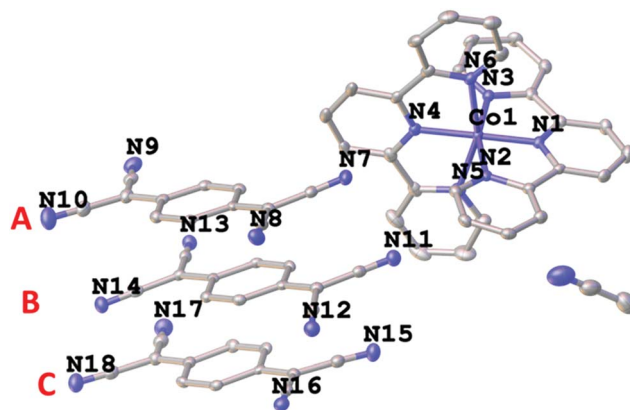

Fig. 1 The asymmetric unit of the crystal structure of **1** with the thermal ellipsoids drawn at the 50% probability level. Hydrogen atoms are omitted for the sake of clarity.

short as compared to those in other LS Co(II) compounds, which is attributed to a strain effect and a stronger Jahn–Teller distortion exerted by the crystal packing effects.[10a,17] As the temperature decreases from 300 K, the Co–N bond lengths do not exhibit a significant decrease until 190 K, which is most likely due to dynamic disorder of HS and LS Co(II) entities.[17a] From 190 to 180 K, when the dynamic disorder diminishes and Co(II) ions are all in the LS state (*vide infra*), an obvious decrease in the Co–N bond distances is observed (Fig. 3a). From 180 to 150 K, four of the Co–N (N1, 4, 5, 6) bonds exhibit an unusual elongation (Fig. 3a) instead of a contraction, which is ascribed to the Jahn–Teller distortion of the ^{2}E state of LS Co(II) ions. This unusual structural "breathing" behavior is also transmitted to the macro-scale as evidenced by a similar trend in all three unit cell axes and the unit cell volume variations (Fig. 3b) upon thermal fluctuation.
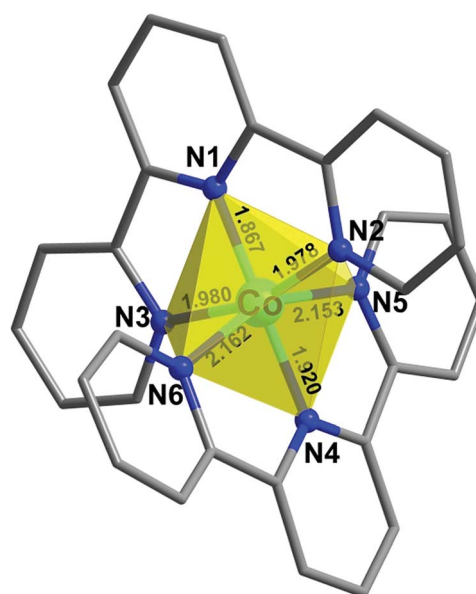

Fig. 2 The coordination sphere of Co(II) in **1** with the Co–N bond distances reported in Å at 100 K.
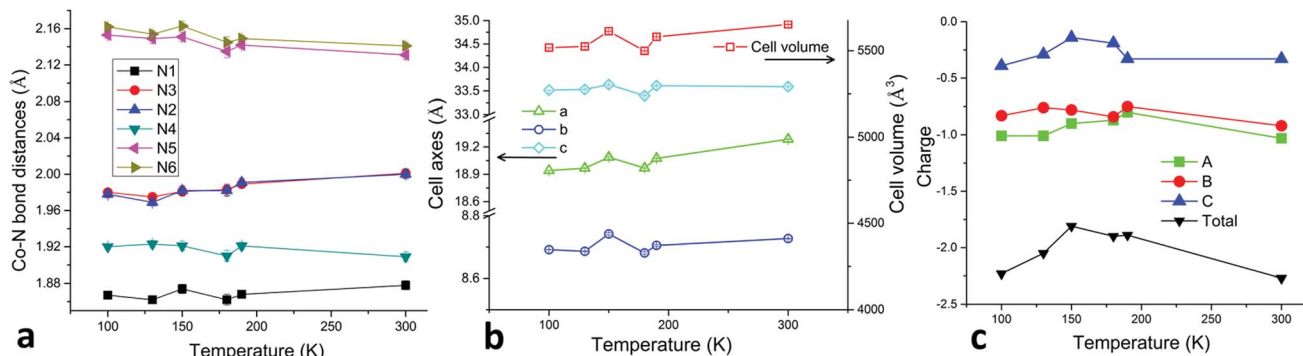
Fig. 3 (a) Temperature dependence of the Co−N bond distances with corresponding error bars for compound **1**. (b) Temperature dependence of the unit cell parameters and volumes with corresponding error bars of compound **1**. (c) Temperature dependence of the estimated charges on individual TCNQ species (A, B, C as denoted in Fig. 1) and the total charge of TCNQ triads.

The TCNQ radicals form triads (ABC as designated in Fig. 1) in the structure, which are then stacked in such a manner that the adjacent triads form a hitherto unknown cross-stacking pattern of TCNQ moieties along the a axis, with a parallel arrangement along the b axis (Fig. 4a and b and S1†). At 180 K, A and B exhibit a close centroid–centroid distance of ~3.35 Å within the triad whereas the centroid–centroid distance between B and C is ~3.77 Å. The corresponding *inter*-triad distances are longer at ~5.52 and 5.57 Å (Fig. 4c). The semi-conducting/SCO layers pack along the c axis in an alternating fashion. The stacking distances of the TCNQ units follow the same trend upon thermal perturbation as the Co–N (N1, 4, 5, 6) bond lengths and a decrease in the centroid–centroid and shift distances from 190 to 180 K was observed (Fig. S3†). The charges on the TCNQ species have been estimated from Kistenmacher's formula based on several signature C–C bond lengths in TCNQ (Table S5†).[18] At 300 K, the negative charges on A (−1.03) and B (−0.92) are close to −1 whereas C (−0.33) is closer to the neutral form. Importantly, the charges on the different TCNQ species fluctuate as the temperature changes (Fig. 3c). From 190 to 180 K, the charges on A and B show a decrease toward −1 while that on C exhibits an increase toward the neutral form to result in a charge localized state of the triads.

Melby and coworkers reported that the charges of the TCNQ species in $[Et_3NH](TCNQ)_2$ are delocalized in the solid state. In solution, the salt dissociates into TCNQ and TCNQ$^{·−}$.[19] Therefore, when employed as a starting material for the current study, $[Et_3NH](TCNQ)_2$ serves as a single source of both neutral and −1 charged TCNQ species for the triads $[(TCNQ)(TCNQ^{·−})_2]^{2−}$ with two of the TCNQ charges (A and B) being close to −1 and that of the third one (C) being nearly 0. A delocalized state is observed in the solid state of **1** close to room temperature.

The temperature dependent magnetic susceptibility of **1** was measured under a 1000 Oe DC magnetic field for $T = 2$–390 K (Fig. 5). A typical Co(II) gradual SCO occurs,[16,20] with $\chi_M T$ gradually decreasing from 1.02 emu K mol^{-1} at 390 K to 0.41 emu K mol^{-1} at 2 K. Even at 390 K the HS state is not fully populated, as the expected $\chi_M T$ value for isolated spin-only HS Co(II) centers is ~1.88 emu K mol^{-1}. The $\chi_M T$ values in the range 190–180 K indicate that nearly all of the Co(II) centers are in the LS state. The TCNQ radicals give rise to a negligible contribution to the magnetic susceptibility which is typical of TCNQ materials due to radical dimerization.[21] No thermal hysteresis was observed.

The temperature dependence of the electrical conductivity of compound **1** was measured on single crystals using the standard four-probe method[22] along the a axis (the TCNQ triad
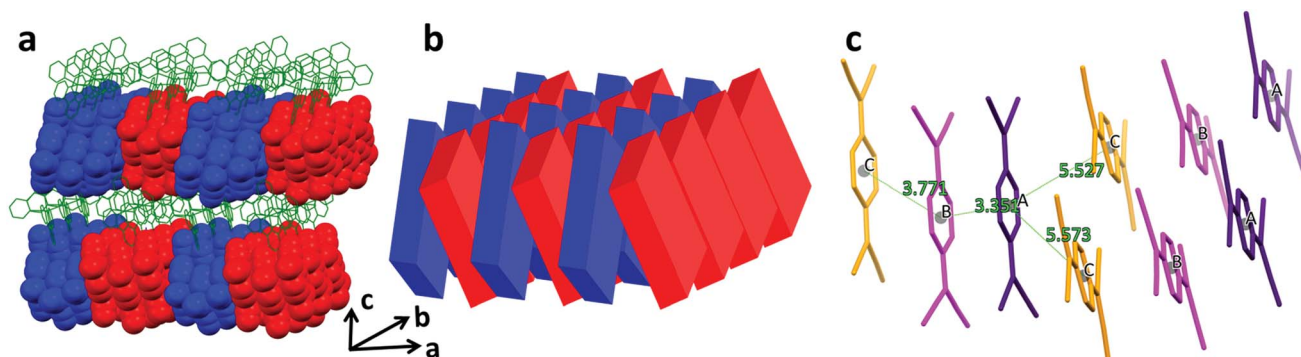

Fig. 4 (a) Packing diagram of the structure of 1. The TCNQ triads (blue and red) are depicted in a space-filling model and the [Co(terpy)$_2$]$^{2+}$ cations (green) and interstitial CH$_3$CN molecules (black) are represented by the capped-stick models. (b) Schematic representation of the "criss-cross" pattern of the TCNQ triads. Each of the colored blocks represents one TCNQ triad. (c) Schematic representation of the *intra*- and *inter*-triad interactions at 180 K. The three distinct TCNQ species are A (purple), B (magenta) and C (orange). The centroid–centroid distances between the quinoid ring centroids of the neighboring TCNQ species are depicted in green.
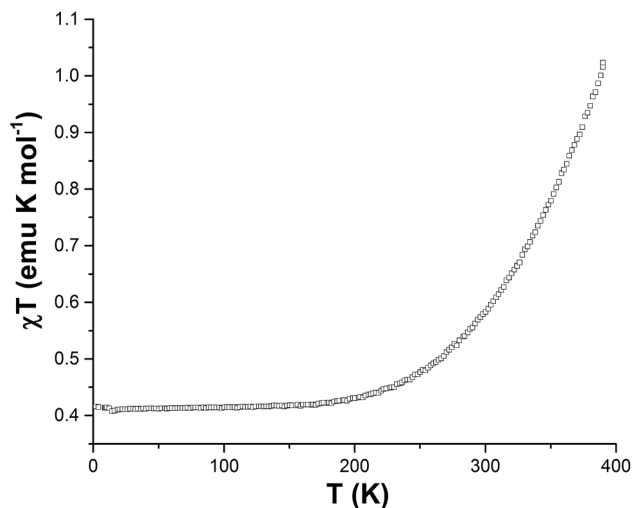
Fig. 5 Temperature dependence of the molar magnetic susceptibility χT product of compound **1**.

stacking direction, Fig. S2†) over the temperature range of 50–300 K. As is expected for partially charged radical stacks of TCNQ,[23] compound **1** exhibits a high room temperature conductivity of 0.13 S cm^{-1} and behaves as a semiconductor between 300 and ∼195 K with a band gap of 0.47 eV (Fig. 6 and S4†). What is most striking, however, is that the conductivity exhibits an unprecedented anomaly with a dip to ∼4.9 × 10^{-7} S cm^{-1} at ∼180 K from ∼8.8 × 10^{-4} S cm^{-1} at ∼190 K (Fig. 6). This anomaly at 180–190 K is attributed to a combination of the TCNQ radical stacking distance variations (Fig. S3†) and charge fluctuations (Fig. 2c) as the temperature decreases from 190 to 180 K. The decrease in the TCNQ stacking distances from 190 to 180 K is correlated to the decrease in Co–N bond distances as well as to a possible Peierls distortion.[24] At the same time, the charge fluctuations of the TCNQ species result in a charge localized state of the TCNQ triads ([[(TCNQ)(TCNQ$^{\bullet-}$)$_2$]$^{2-}$) at 180
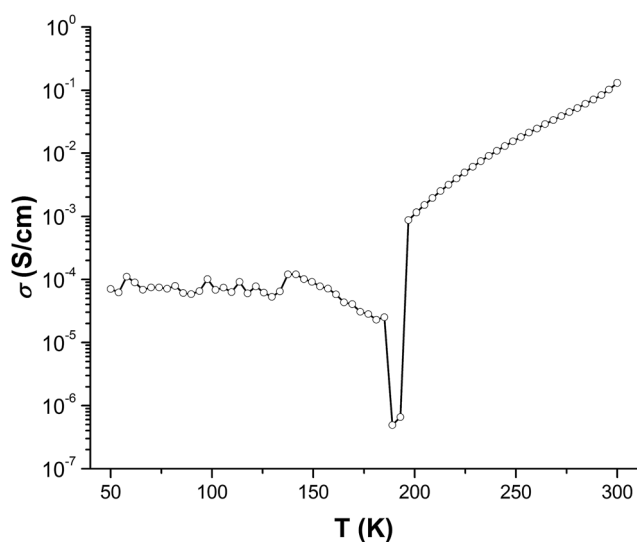
K that also contributes to the decrease in conductivity, as the charges on A and B become close to −1 and C is in the neutral form (*vide supra*). Below 150 K, the conductivity becomes nearly independent of temperature until 50 K which is also likely a result of the Peierls state but with slightly larger stacking distances than those at 180 K. Besides the stacking interactions of the TCNQ moieties within the triads, the cross-stacking pattern of the TCNQ triads is also likely to be important for the conducting behavior as it disrupts continuous overlap of the frontier orbitals and at the same time minimizes Coulomb repulsion between adjacent triads. Obviously, a precise understanding of the role of the inter-triad interactions for charge transport requires in-depth theoretical studies.

Experimental

The starting materials (Et$_3$NH)(TCNQ)$_2$ and Co(terpy)$_2$(ClO$_4$)$_2$·0.5H$_2$O were synthesized according to the literature procedures.[19,25] **Caution!** Perchlorates are potentially explosive and should be handled very carefully in small amounts. Avoid heat, drying and grinding.

A solution of (Et$_3$NH)(TCNQ)$_2$ (0.15 mmol) in MeCN (9 mL) was added to a solution of Co(terpy)$_2$(ClO$_4$)$_2$·0.5H$_2$O (0.1 mmol) in MeCN (2 mL). After several minutes, X-ray quality dark blue needles of **1** had already formed. The product was separated by filtration after 30 min. Yield 50.7 mg (45%). Elemental analysis: calculated (%) for Co$_1$C$_{66}$N$_{18}$H$_{34}$·CH$_3$CN: C(69.27), H(3.16), N(22.57); found: C(69.15), H(3.64), N(22.43). IR: Nujol mulls on KBr plates: ν (CN) 2200.1, 2171.1 and 2152.3 cm^{-1}, δ (C–H, TCNQ) 834.0 and 823.7 cm^{-1}.

Magnetic measurements were carried out using a Quantum design MPMS-XL SQUID instrument over the temperature range 2–390 K. The diamagnetic contributions of the atoms and sample holders were accounted for during the data analysis process by using Pascal's constants.

A standard four-probe method was used to measure the resistivity with gold wires attached to the thin needle-like single crystals using gold paste. The measurements were carried out on multiple samples and the general profile of temperature dependent conductivity is exemplified by Fig. 6. The temperature was controlled by using the cryogenics of a SQUID MPMS instrument at a rate of 2 K min^{-1} and stabilized at each point for 60 s before the next measurement was made to allow for thermal equilibration of the samples.

Conclusions

In summary, an anomalous conducting behavior occurs at 180–190 K in a highly conducting hybrid inorganic/organic-radical bifunctional SCO conducting molecular material. This anomaly is directly correlated with the structural variation arising from the HS to LS transition of Co(II), subsequent Jahn–Teller distortion of LS Co(II) and concomitant charge fluctuations of the partially charged TCNQ radicals. This modular synthetic procedure for the introduction of partially charged TCNQ radicals is highly promising for the synthesis of other

Fig. 6 Temperature dependence of the electrical conductivity of compound **1**.

bifunctional materials with electrical conducting properties, efforts that are currently being explored in our laboratories.

Acknowledgements

Notes and references

1 (a) K. G. Sharp, *Adv. Mater.*, 1998, **10**, 1243–1248; (b) C. R. Kagan, D. B. Mitzi and C. D. Dimitrakopoulos, *Science*, 1999, **286**, 945–947; (c) C. Draxl, D. Nabok and K. Hannewald, *Acc. Chem. Res.*, 2014, **47**, 3225–3232; (d) P. Judeinstein and C. Sanchez, *J. Mater. Chem.*, 1996, **6**, 511–525; (e) J. S. Miller, A. J. Epstein and W. M. Reiff, *Science*, 1988, **240**, 40–47.

2 (a) G. Christou, D. Gatteschi, D. N. Hendrickson and R. Sessoli, *MRS Bull.*, 2000, **25**, 66–71; (b) W.-X. Zhang, R. Ishikawa, B. Breedlove and M. Yamashita, *RSC Adv.*, 2013, **3**, 3772–3798; (c) E. Coronado, A. Forment-Aliaga, J. R. Galán-Mascarós, C. Giménez-Saiz, C. J. Gómez-García, E. Martinéz-Ferrero, A. Nuez and F. M. Romero, *Solid State Sci.*, 2003, **5**, 917–924.

3 E. Coronado, C. Giménez-Saiz and C. Martí-Gastaldo, in *Engineering of Crystalline Materials Properties*, ed. J. Novoa, D. Braga and L. Addadi, Springer, Netherlands, 2008, pp. 173–191.

4 (a) E. Coronado, J. R. Galan-Mascaros, C. J. Gomez-Garcia and V. Laukhin, *Nature*, 2000, **408**, 447–449; (b) K. Kazuya, H. Hiroki, M. Hitoshi and Y. Masahiro, in *Multifunctional Molecular Materials*, Pan Stanford Publishing, 2013, pp. 61–103.

5 (a) Z.-Y. L. Osamu Sato, Z.-S. Yao, S. Kang and S. Kanegawa, in *Spin-Crossover Materials: Properties and Applications*, ed. M. A. Halcrow, John Wiley & Sons, Ltd, 2013; (b) W. Xue, B. Y. Wang, J. Zhu, W. X. Zhang, Y. B. Zhang, H. X. Zhao and X. M. Chen, *Chem. Commun.*, 2011, **47**, 10233–10235.

6 (a) A. Pearson, R. Ramanathan, A. P. O'Mullane and V. Bansal, *Adv. Funct. Mater.*, 2014, **24**, 7570–7579; (b) A. Nafady, A. P. O'Mullane and A. M. Bond, *Coord. Chem. Rev.*, 2014, **268**, 101–142; (c) H. Fukunaga and H. Miyasaka, *Angew. Chem., Int. Ed. Engl.*, 2015, **54**, 569–573; (d) A. A. Talin, A. Centrone, A. C. Ford, M. E. Foster, V. Stavila, P. Haney, R. A. Kinney, V. Szalai, F. El Gabaly, H. P. Yoon,

F. Léonard and M. D. Allendorf, *Science*, 2014, **343**, 66–69; (e) M. Nishio, N. Hoshino, W. Kosaka, T. Akutagawa and H. Miyasaka, *J. Am. Chem. Soc.*, 2013, **135**, 17715–17718; (f) K. E. Knowles, M. Malicki, R. Parameswaran, L. C. Cass and E. A. Weiss, *J. Am. Chem. Soc.*, 2013, **135**, 7264–7271; (g) M. Garnica, D. Stradi, S. Barja, F. Calleja, C. Diaz, M. Alcami, N. Martin, A. L. Vazquez de Parga, F. Martin and R. Miranda, *Nat. Phys.*, 2013, **9**, 368–374; (h) Z. Zhang, H. Zhao, M. M. Matsushita, K. Awaga and K. R. Dunbar, *J. Mater. Chem. C*, 2014, **2**, 399–404; (i) Z. X. Wang, X. Zhang, Y. Z. Zhang, M. X. Li, H. Zhao, M. Andruh and K. R. Dunbar, *Angew. Chem., Int. Ed.*, 2014, **53**, 11567–11570; (j) S. Shimomura and S. Kitagawa, *J. Mater. Chem.*, 2011, **21**, 5537–5546; (k) J. S. Miller, *Chem. Soc. Rev.*, 2011, **40**, 3266–3296; (l) E. B. Vickers, T. D. Selby, M. S. Thorum, M. L. Taliaferro and J. S. Miller, *Inorg. Chem.*, 2004, **43**, 6414–6420; (m) J. S. Miller, J. H. Zhang, W. M. Reiff, D. A. Dixon, L. D. Preston, A. H. Reis, E. Gebert, M. Extine, J. Troup, *et al.*, *J. Phys. Chem.*, 1987, **91**, 4344–4360; (n) X. Zhang, M. R. Saber, A. P. Prosvirin, J. H. Reibenspies, L. Sun, M. Ballesteros-Rivas, H. Zhao and K. R. Dunbar, *Inorg. Chem. Front.*, 2015, **2**, 904–911; (o) X. Zhang, Z. Zhang, H. Zhao, J. G. Mao and K. R. Dunbar, *Chem. Commun.*, 2014, **50**, 1429–1431.

7 (a) A. F. Garito and A. J. Heeger, *Acc. Chem. Res.*, 1974, **7**, 232–240; (b) T. Mori, *Chem. Rev.*, 2004, **104**, 4947–4970.

8 (a) R. Clérac, S. O'Kane, J. Cowen, X. Ouyang, R. Heintz, H. Zhao, M. J. Bazile and K. R. Dunbar, *Chem. Mater.*, 2003, **15**, 1840–1850; (b) M. Ballesteros-Rivas, A. Ota, E. Reinheimer, A. Prosvirin, J. Valdes-Martinez and K. R. Dunbar, *Angew. Chem., Int. Ed.*, 2011, **50**, 9703–9707.

9 (a) M. A. Halcrow, *Chem. Commun.*, 2013, **49**, 10890–10892; (b) P. Gütlich, A. B. Gaspar and Y. Garcia, *Beilstein J. Org. Chem.*, 2013, **9**, 342–391; (c) P. Gütlich, *Eur. J. Inorg. Chem.*, 2013, 581–591.

10 (a) K. Takahashi, H.-B. Cui, Y. Okano, H. Kobayashi, H. Mori, H. Tajima, Y. Einaga and O. Sato, *J. Am. Chem. Soc.*, 2008, **130**, 6688–6689; (b) M. Nihei, N. Takahashi, H. Nishikawa and H. Oshio, *Dalton Trans.*, 2011, **40**, 2154–2156.

11 (a) A. Hauser, J. Jeftić, H. Romstedt, R. Hinek and H. Spiering, *Coord. Chem. Rev.*, 1999, **190–192**, 471–491; (b) M. A. Halcrow, *Coord. Chem. Rev.*, 2009, **253**, 2493–2514.

12 (a) Y.-S. Koo and J. R. Galán-Mascarós, *Adv. Mater.*, 2014, **26**, 6785–6789; (b) Y.-C. Chen, Y. Meng, Z.-P. Ni and M.-L. Tong, *J. Mater. Chem. C*, 2015, **3**, 945–949.

13 (a) S. Dorbes, L. Valade, J. A. Real and C. Faulmann, *Chem. Commun.*, 2005, 69–71; (b) C. Faulmann, K. Jacob, S. Dorbes, S. Lampert, I. Malfant, M.-L. Doublet, L. Valade and J. A. Real, *Inorg. Chem.*, 2007, **46**, 8548–8559; (c) K. Takahashi, H.-B. Cui, Y. Okano, H. Kobayashi, Y. Einaga and O. Sato, *Inorg. Chem.*, 2006, **45**, 5739–5741.

14 (a) M. Nakano, N. Fujita, G.-E. Matsubayashi and W. Mori, *Mol. Cryst. Liq. Cryst.*, 2002, **379**, 365–370; (b) H. Phan, S. M. Benjamin, E. Steven, J. S. Brooks and M. Shatruk, *Angew. Chem., Int. Ed.*, 2015, **54**, 823–827.

15 C. Alonso, L. Ballester, A. Gutiérrez, M. F. Perpiñán, A. E. Sánchez and M. T. Azcondo, *Eur. J. Inorg. Chem.*, 2005, 486–495.

16 X. Zhang, H. Xie, M. Ballesteros-Rivas, Z.-X. Wang and K. R. Dunbar, *J. Mater. Chem. C*, 2015, **3**, 9292–9298.

17 (a) C. A. Kilner and M. A. Halcrow, *Dalton Trans.*, 2010, **39**, 9008–9012; (b) A. L. Reiff, E. M. Garcia-Frutos, J. M. Gil, O. P. Anderson and L. S. Hegedus, *Inorg. Chem.*, 2005, **44**, 9162–9174.

18 T. J. Kistenmacher, T. J. Emge, A. N. Bloch and D. O. Cowan, *Acta Crystallogr., Sect. B: Struct. Crystallogr. Cryst. Chem.*, 1982, **38**, 1193–1199.

19 L. R. Melby, R. J. Harder, W. R. Hertler, W. Mahler, R. E. Benson and W. E. Mochel, *J. Am. Chem. Soc.*, 1962, **84**, 3374–3387.

20 (a) R. G. Miller and S. Brooker, *Inorg. Chem.*, 2015, **54**, 5398–5409; (b) S. Hayami, Y. Komatsu, T. Shimizu, H. Kamihata and Y. H. Lee, *Coord. Chem. Rev.*, 2011, **255**, 1981–1990.

21 (a) H. Oshio, E. Ino, I. Mogi and T. Ito, *Inorg. Chem.*, 1993, **32**, 5697–5703; (b) A. M. Madalan, H. W. Roesky, M. Andruh, M. Noltemeyer and N. Stanica, *Chem. Commun.*, 2002, 1638–1639; (c) H. Kubota, Y. Takahashi, J. Harada and T. Inabe, *Cryst. Growth Des.*, 2014, **14**, 5575–5584.

22 G. Givaja, P. Amo-Ochoa, C. J. Gomez-Garcia and F. Zamora, *Chem. Soc. Rev.*, 2012, **41**, 115–147.

23 (a) T. Ikari, S. Jandl, M. Aubin and K. D. Truong, *Phys. Rev. B*, 1983, **28**, 3859–3863; (b) A. R. Blythe, M. R. Boon and P. G. Wright, *Discuss. Faraday Soc.*, 1971, **51**, 110–115; (c) K. Holczer, G. Mihaly, A. Janossy, G. Gruner and M. Kertesz, *J. Phys. C: Solid State Phys.*, 1978, **11**, 4707.

24 L. B. Coleman, M. J. Cohen, D. J. Sandman, F. G. Yamagishi, A. F. Garito and A. J. Heeger, *Solid State Commun.*, 1973, **12**, 1125–1132.

25 S. Kremer, W. Henke and D. Reinen, *Inorg. Chem.*, 1982, **21**, 3013–3022.